Academia Journal of Scientific Research 5(11): 000-000, November 2017
DOI: 10.15413/ajsr.2017.0722
ISSN 2315-7712

Research Paper

Synthesis of aluminum carbide/carbon nanotube for electrodes in aluminum capacitors

Accepted 18th November, 2017

Chuen-Chang Lin*, Nai-Gang Rao and Wei-Chieh Peng

Department of Chemical And Materials Engineering, National Yunlin University of Science and Technology, 123 University Road Sec. 3, Douliu, Yunlin 64002, Taiwan.

*Corresponding author. E-mail: linchuen@yuntech.edu.tw. Tel: +886-5-534-2601 Ext. 4619; Fax: +886-5-531-2071.

ABSTRACT

Carbon nanotubes (CNTs) were directly grown on cobalt-coated aluminum foil by chemical vapor deposition. They were subsequently grown within the carbon nanotube aluminum foil electrodes by chemical vapor deposition at different temperatures and durations with aluminum powder/graphite powder and/or CH_4. Thus, negative electrodes were obtained. Subsequently, alumina was deposited onto aluminum carbide grown within carbon nanotube aluminum foil by a chemical liquid phase deposition method and positive electrodes were obtained. Finally, a negative electrode coated with solid conducting polymer electrolyte (poly-3, 4-ethylenedioxythiophene) was assembled with a positive electrode into an aluminum capacitor. The capacitance for aluminum carbide grown at 590°C was lower than that of aluminum carbide grown at 540°C. Furthermore, the decreasing rate of capacitance for aluminum carbide grown for one hour was lower than that of aluminum carbide grown for three or five hours. The decreasing rate of capacitance for aluminum carbide grown with aluminum powder/graphite powder and CH_4 was lower than the others examined.

Keywords: Aluminum carbide, chemical vapor deposition, aluminum capacitors.

INTRODUCTION

Aluminum electrolytic capacitors have been widely used as power supplies for all types of electronic equipment including automobiles, computers, monitors and other electronic components. The aluminum electrolytic capacitor consists of aluminum anode foil - on which an oxide is prepared by an electrochemical oxidation process - a suitable electrolyte and aluminum cathode foil. The capacitance of the aluminum cathode foil is much higher than the aluminum anode foil such that the applied potential appears mainly on the aluminum anode foil, which determines operation potential and capacitance (Goad and Uchi, 2000; Kang et al., 2005). Thus, we were concerned principally with the anode electrode. In order to improve the adhesion of carbon nanotubes (CNTs) and then enhance operational stability of aluminum capacitors, an interposition layer (aluminum carbide) was formed in this study.

CNTs quickly rise to the surface and do not participate in the chemical reaction as a result of the poor wetting properties of CNTs and differences in their densities when CNTs are mixed into melting Al. However, the Al before or after melting reacts with carbon due to negative free energy of Gibss (Chunfeng et al., 2007). Due to relatively low free energy of Gibss (-12.7 kcal at 298 K), aluminum carbide is easily formed at the interface of Al as well as, CNT layers and reactions generally occur at locations containing an amorphous carbon coating at defect sites and at open ends of CNTs (Ci et al., 2006).

The formation of aluminum carbide is confined to the Al/nanotube interface and CNTs synthesized by chemical vapor deposition (CVD) have a few defects as well as significant amorphous carbon coating on the tube surface, which promote the precipitation of an Al_4C_3 layer (He et al., 2009). CNTs synthesized by CVD as well as Al powder were heat-treated to form aluminum carbide at different temperatures (800 to 1250°C) and the amorphous carbon layer initially reacted homogenously at the CNT surface to form a uniform Al_4C_3 film. Reactions may be limited by diffusion through this film. However, at sufficiently high temperature, this film continued to grow until an Al_4C_3 nanowire was produced (He et al., 2010). Two different types (dumbbell and tube) of aluminum carbide were observed in the boundary zone and dumbbell-shaped Al_4C_3 originated from the CNT tips, whereas tube-shaped Al_4C_3 originated from defective CNTs (Kwon et al., 2010). Aluminum carbide did not form during the mechanical alloying process and the milled (20 mm steel balls, ball-to-powder weight ratio = 10/1 and 600 rpm of rotational speed) powder was then annealed at temperatures higher than 300°C in order to form Al_4C_3, which increased with increasing annealing temperatures. High defect due to the formation of nanostructure aluminum as well as the nanocrystalline carbon produced during milling can ensure large reaction interface areas between C and Al enhance their diffusion rates through aluminum carbide causing a decrease in the reaction temperatures (Sharifi et al., 2012).

CNTs were first milled (0 to 5 h and 1200 rpm) alone, thereafter, a mixture of 10 volume % CNT/Al was also milled (2 wt. % stearic acid added as a process-control agent to avoid excessive sticking as well as, agglomeration of Al for 0.5 to 5 h and 1200 rpm in an Ar atmosphere) and the milled powder was annealed at 630°C under vacuum for one hour (Poirier et al., 2009). A mixture of Al powder (48.5 g, 99% purity, 150 μm maximum particle size) and carbon black (1.5 g, 99% purity, 2.4 μm mean particle size) was mechanically alloyed (10 mm steel balls, ball-to-powder weight ratio = 6/1.2 wt. % process control agent added, 20 h and 450 rpm in an Ar atmosphere) and the milled powder annealed at 650°C for twenty hours (Arik et al., 2006). C_{60} powder (98%) and two Al sheets (99.95%) were used as carbon and Al sources, respectively. C_{60} possessed higher activity and a lower sublimation temperature in comparison with other carbon materials. When the system was annealed to 350°C, plenty of C_{60} molecules sublimated and deposited onto the Al microballs (1 to 2 μm), which were covered by a tungsten foil (99.9%) that was used as a substrate to form a high quality textured C_{60} thin film with many nanoholes. With the temperature increasing, the textured C_{60} thin film was prone to amorphization because of the existence of residual oxygen in the system and then reacted with Al to form aluminum carbide textured thin film (Sun et al., 2011).

In order to improve the adhesion between an active substance layer (carbon-containing) and aluminum materials, interposition layers (Al_4C_3) were formed between the carbon-containing layer and the aluminum materials by different hydrocarbon-containing substances (C_2H_2, CH_4, C_2H_2+Ar and CH_4+Ar), at temperatures of 540, 590 and 620°C for 10 and 60 h, respectively. The resulting materials were then annealed at 620°C for 2 h (Ro and Ashitaka, 2005; Ro et al., 2009).

Carbon-coated aluminum nanopowders were synthesized by laser-induction plasma arc heating (bulk pure Al melted and then vaporized) as well as pyrolysis of methane and simultaneously Al_4C_3 was formed (Guo et al., 2007). Al-CNT composites were fabricated by hot-pressing of the 1 wt. % and 4 wt. %, as well as 10 wt. % CNTs and 35 g Al powder and simultaneously AlC or AlC_2 was formed (Xu et al., 1999).

The aluminum composite dispersion strengthened by Al_4C_3 particles was prepared by mechanical alloying and the carbide content was in the range of 2.5 to 12 vol. % (Besterci, 2006a). Al_4C_3 precipitation starts when the Al/C powder is milled at least 6 h as well as, heated until 550°C and the volume fraction of Al_4C_3 increases with increasing milling time (Birol, 2008). The transformation efficiency (100%) of carbon to Al_4C_3 by heat treatment (3 h and 550°C) of Al powder with porous furnace black (a_1) is higher than that of the hard cracked graphite since the porous carbon type is incorporated into the matrix by friction during milling; its distribution is even and clustering is small; however, the hard graphite resists disintegration and the granules are large (Besterci, 2006b).

The transformation efficiency (dependent on temperature, hold time and carbon type) of carbon to Al_4C_3 by heat treatment (550°C and 3 h) of Al with the porous furnace black (made by incomplete burning of carbohydrates at low temperatures) could reach about 100% and the homogeneity of carbide distribution as well as, the amount of contact surface area would influence the transformation kinetics of Al+C into aluminum carbide (Besterci, 2006a).

In the polyester binder-assisted (PBA) method, polyethylene glycol was expected to both disperse and bind CNTs on Al powder surface. The number of defects apparently increased in the CNTs after high energy ball-milling and the CNT dispersion in the high energy ball-milled sample was better than that in low energy ball-milled or PBA samples (Liao and Tan, 2011). When aluminum foil (99.3% and 50 μm thickness) was annealed at 823 K for 25 ks in a hydrocarbon gas atmosphere, aluminum carbide was formed as a result of the chemical reaction between aluminum and carbon at the interface and the whiskers generated on the aluminum carbide cores successfully fixed carbon particles on the aluminum foil without any binder (Lu et al., 2004a). The carbon particles (~1 μm in diameter) were stucked to aluminum carbide whiskers strongly and substantially, the whiskers as well as, aluminum foil seem to be one body and the capacitance of the material increased with the thickness of the carbon layer (Lu et al., 2004b).

The most important parameter influencing the growth rate and the amount of aluminum carbide is infiltration temperature. The degree of graphitization of the carbon fibers determines the fiber's reactivity to the heterogeneous nucleation of aluminum carbide which is associated with surface defects on carbon fibers, for example, exposed edges of graphite basal planes that exhibit carbon atoms with uncompensated high energy electron bonds (Etter et al., 2007).In order to find better cyclic stability and capacitance of aluminum capacitors, aluminum carbide was grown within carbon nanotube aluminum foil electrodes by chemical vapor deposition at different temperatures as well as, durations with aluminum powder/graphite powder and/or CH_4 in this research.

MATERIALS and METHODS

Aluminum foil (10 × 5 × 0.001 cm^3, purity 99.98%) decreased in acetone for 5 min. In order to remove the oxide layer from its surface, it was then immersed in 1 M aqueous NaOH for 2 min and subsequently rinsed with de-ionized water. Next, it was rinsed ultrasonically with alcohol for 15 min.

Before carbon nanotube growth, the cobalt (Co) catalyst particles were electrochemically deposited on the pretreated aluminum foil in an electrolyte of $CoSO_4 \cdot 7H_2O$ (5 wt. %) and H_3BO_3 (2 wt. %) by applying an alternating current potential of 10.5 V (frequency: 60 Hz) for 60 s. Next, CNTs were grown on the Co-coated aluminum foil using thermal CVD with the gas mixture (C_2H_2 = 50 sccm and Ar =100 sccm) at 600°C for 60 min.In order to improve the adhesion of CNTs, aluminum powder (0 and 3 g), graphite powder (0 and 3 g) and binder (0 and 1.5 g polyethylene terephthalate) were dispersed in toluene solvents (0 and 22.44 ml) to obtain coating solutions which were applied to the CNT surfaces with a thickness of 10 μm and then oven-dried in air at 100°C for 15 min. Next, aluminum carbide was grown within carbon nanotube aluminum foil by chemical vapor deposition at different temperatures (540 and 590°C) as well as, durations (1, 3 and 5 h) under CH_4 (0 and 100 sccm) atmosphere and subsequently annealed in air at 300°C for 2 h. Thus, negative electrodes of aluminum capacitors were obtained.

A saturated solution of $Al_2(SO_4)_3$ was prepared as a source liquid. The suspended particles were hydrolytes of Al^{+3} and could be filtered out by a 0.2 μm filter. Fine sodium bicarbonate powder was added slowly to obtain a pH value of 2.89 for the growth solution. As soon as the reaction was completed, DI water was immediately added in order to increase the pH to 3.80. After being filtered again by a 0.2 μm filter, the solution was then ready for alumina thin film growth on aluminum carbide grown within carbon nanotube aluminum foil for 3 h at ambient temperatures. Aluminum oxide was subsequently annealed in Ar for 30 min at 500°C and positive electrodes of aluminum capacitors obtained.

Finally, a negative electrode coated with solid conducting polymer electrolyte (PEDOT: poly-3, 4-ethylenedioxythiophene) polymerized at 6 to 1 weight ratios: iron (III) *p*-toluene sulfonate hexahydrate-6 H_2O (oxidant) to 3, 4-ethylenedioxythiophene (monomer) was assembled with a positive electrode into an aluminum capacitor by a coin cell manual crimping machine (CR2032, Taiwan).

Capacitance measurements were made at 120 Hz (frequency) with an LCR (inductance, capacitance and resistance) meter (Hioki, 3522-50, Japan). Furthermore, XRD (X-ray diffraction) (MAC SCIENCE, Japan) with low angle of incidence was used to characterize the crystalline structure of aluminum carbide being formed under different growing conditions. In order to observe the structure as well as, the chemical composition of aluminum carbide and the CNT conditions of aluminum carbide grown within carbon nanotube aluminum foil by chemical vapor deposition at different temperatures and durations, a field emission scanning electron microscope (FE-SEM) combined with energy dispersive X-ray (EDX) (JEOL JSM-6700F, Japan) was employed.

RESULTS and DISCUSSION

Figure 1 shows the effects of different temperatures on aluminum carbide grown for one hour (with aluminum powder, graphite powder and CH_4) and differing numbers of charge-discharge cycles on capacitance. The capacitance for aluminum carbide grown at 590°C was lower than that of aluminum carbide grown at 540°C. This behavior may be explained by the fact that the higher the temperature for growing aluminum carbide, the more the amount of CNTs and graphite powder burnt due to binder (polyethylene terephthalate) containing oxygen (Figure 2), thus leading to lower capacitance. Furthermore, the decreasing rate of capacitance for aluminum carbide grown at 540°C was almost equal to that of aluminum carbide grown at 590°C (Figure 1) because of almost the same relative intensity (2Θ = 37.850) of Al_4C_3 for aluminum carbide grown at 540 and 590°C, respectively (Figure 3).

Figure 4 shows the effects of different durations for aluminum carbide grown at 540°C (with aluminum powder, graphite powder and CH_4) and charge-discharge cycles on the capacitance. The longer the duration for growing aluminum carbide, the lower the capacitance (Figure 4) because the longer the duration for growing aluminum carbide, the more the amount of CNTs and graphite powder burnt [binder (polyethylene terephthalate) containing oxygen) (Figure 5), thus, leading to lower capacitance. Furthermore, the decreasing rate of capacitance for aluminum carbide grown for one hour was lower than that of the aluminum carbide grown for three or five hours (Figure 4) due to higher relative intensity (2Θ =37.850) of Al_4C_3 for one hour growth aluminum carbide (Figure 6).

Figure 7 shows the effects of aluminum carbide grown

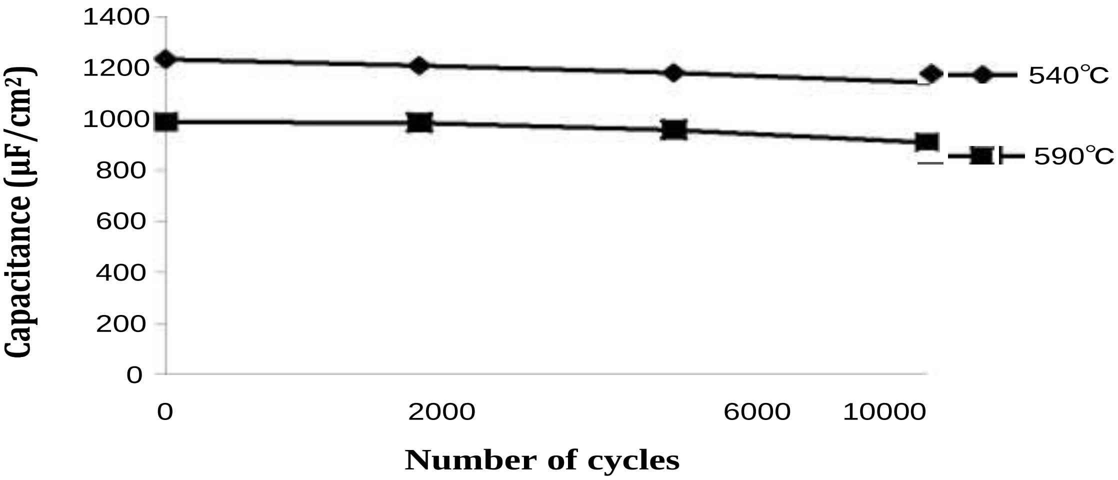

Figure 1: The effects of different temperatures on aluminum carbide grown for one hour (with aluminum powder, graphite powder and CH_4) and differing numbers of charge-discharge cycles on capacitance

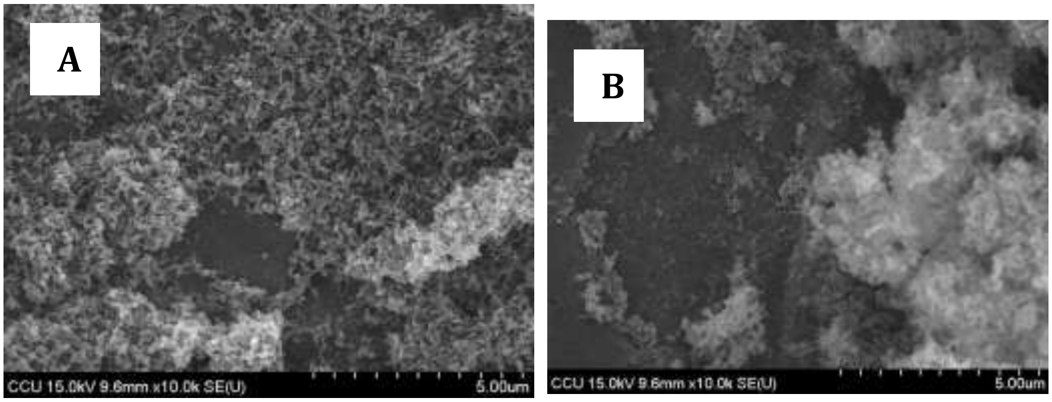

Figure 2: FE-SEM micrographs of aluminum carbide grown for one hour at (a) 540°C and (b) 590°C (with aluminum powder, graphite powder and CH_4).

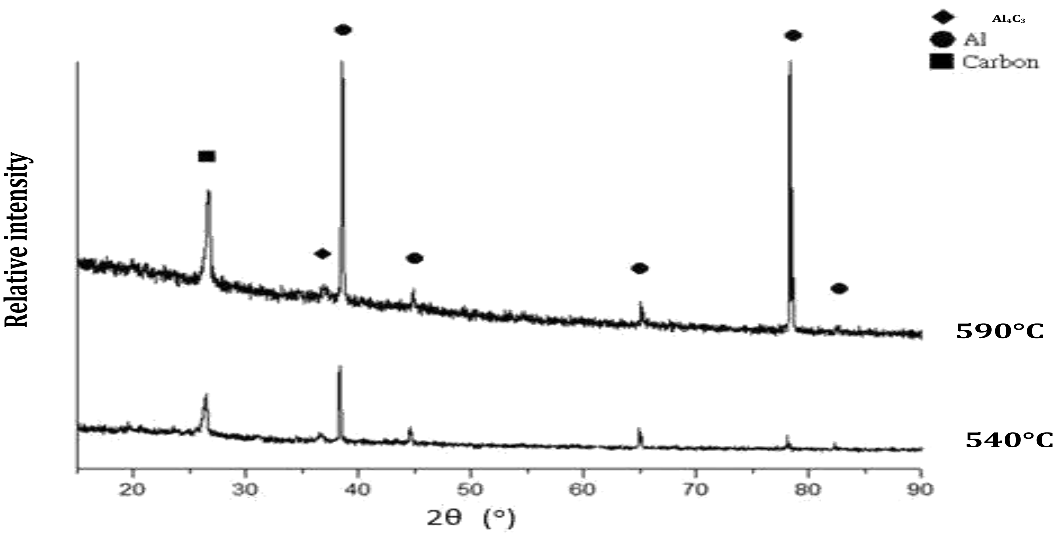

Figure 3: X-ray diffraction patterns of aluminum carbide grown at different temperatures for one hour (with aluminum powder, graphite powder and CH_4).

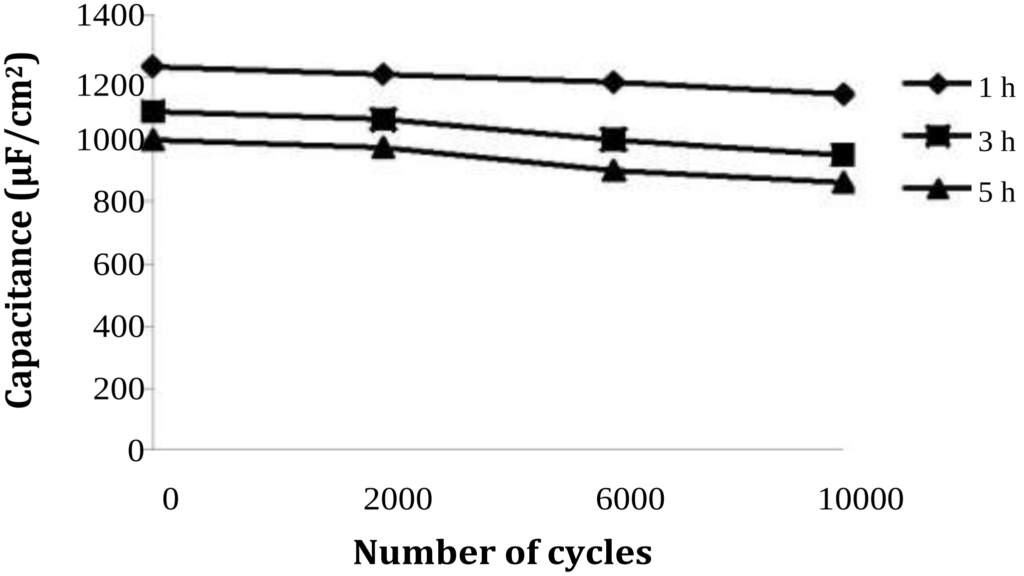

Figure 4: The effects of different durations on aluminum carbide grown at 540°C (with aluminum powder, graphite powder and CH_4) and differing numbers of charge-discharge cycles on capacitance.

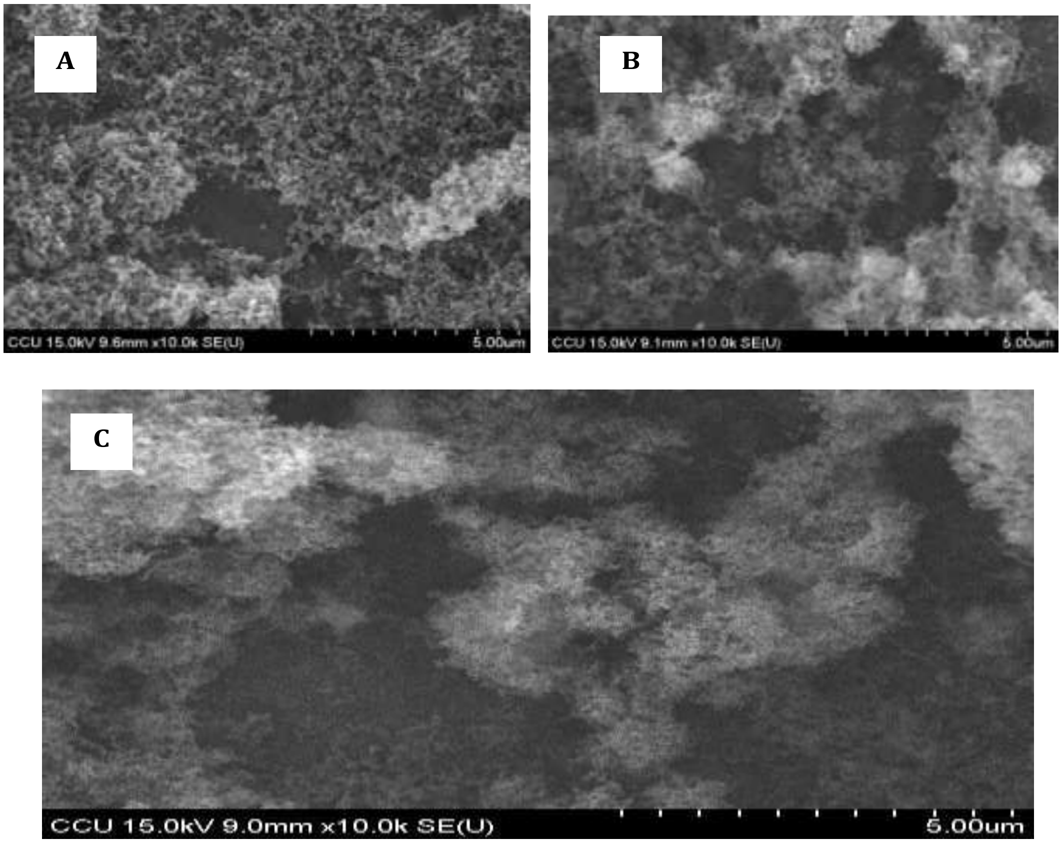

Figure 5: FE-SEM micrographs of aluminum carbide grown for (a) 1 h, (b) 3 h and (c) 5 h at 540°C (with aluminum powder, graphite powder and CH_4).

with aluminum powder/graphite powder and/or CH_4 for 1 h at 540°C and different charge-discharge cycles on the capacitance. The capacitance for aluminum carbide grown only with CH_4 was lower than that of others. The reason

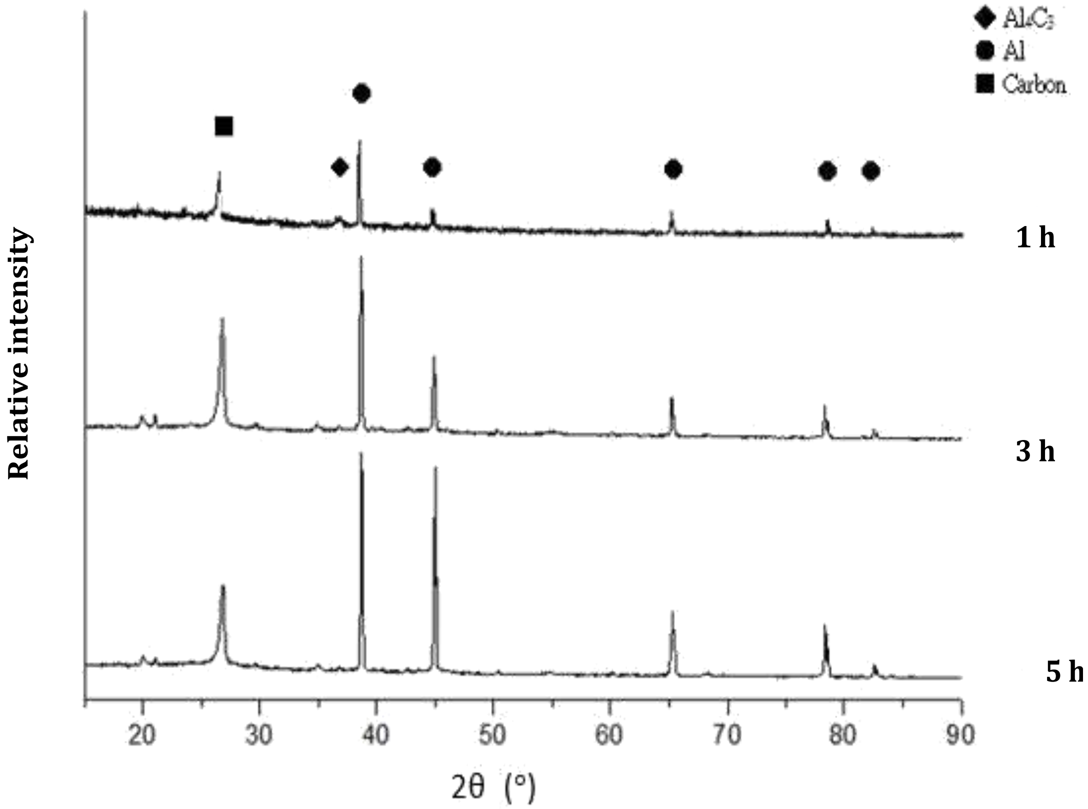

Figure 6: X-ray diffraction patterns of different durations for aluminum carbide grown at 540°C (with aluminum powder, graphite powder and CH_4).

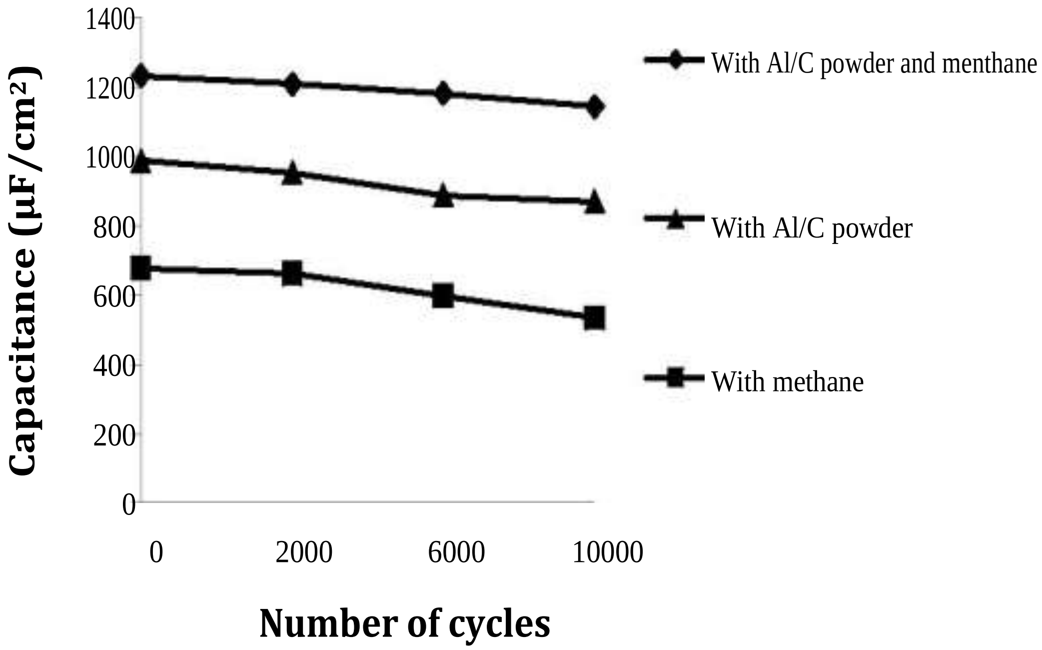

Figure 7: The effects of aluminum carbide grown with aluminum powder/graphite powder and/or CH_4 for 1 h at 540°C and different charge-discharge cycles on the capacitance.

for this may be that graphite powder did not completely react to form aluminum carbide (Figure 8) and thus, the

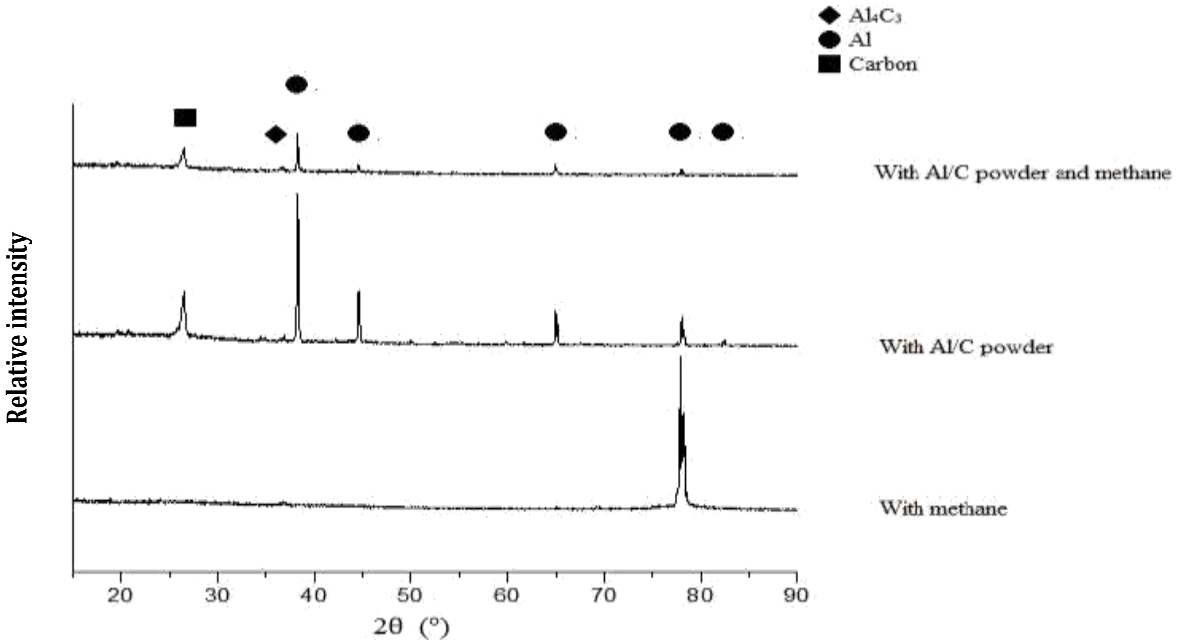

Figure 8: X-ray diffraction patterns of aluminum carbide grown with aluminum powder/graphite powder and/or CH_4 for 1 h at 540°C.

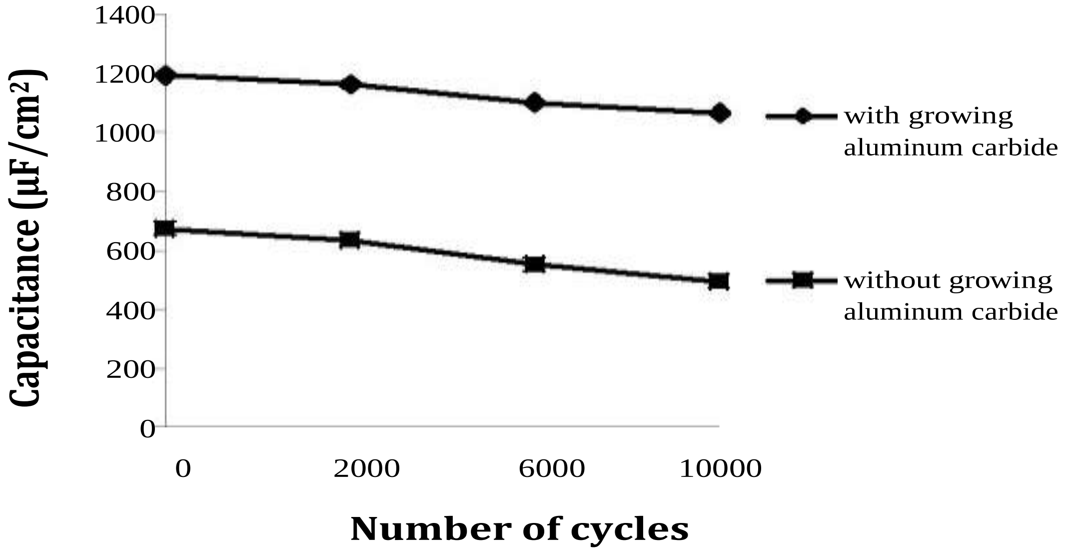

Figure 9: The effects of presence or absence of aluminum carbide (grown with Al powder/C powder and CH_4 for 1 h at 540°C) and different charge-discharge cycles on the capacitance.

remaining graphite powder led to higher capacitance.

Furthermore, the decreasing rate of capacitance for aluminum carbide grown with aluminum powder/graphite powder and CH_4 was lower than that of others (Figure 7) because of higher relative intensity (2Θ = 37.850) of Al_4C_3 for aluminum carbide grown with aluminum powder/graphite powder and CH_4 (Figure 8).

Figure 9 shows the effects of presence or absence of aluminum carbide (grown with Al powder/C powder and CH_4 for 1 h at 540°C) and different charge-discharge cycles on the capacitance. The capacitance with aluminum carbide was higher than that without aluminum carbide. The reason behind this may be that relative intensity (2Θ = 26.50) of carbon growing with aluminum carbide was much higher than that growing without aluminum carbide (Figure 10) due to a small amount of graphite powder being reacted to form aluminum carbide [relative intensity (2Θ = 37.850) of Al_4C_3 in Figure 10 and thus, the remaining graphite powder caused higher capacitance. Furthermore, the decreasing rate of capacitance with aluminum carbide

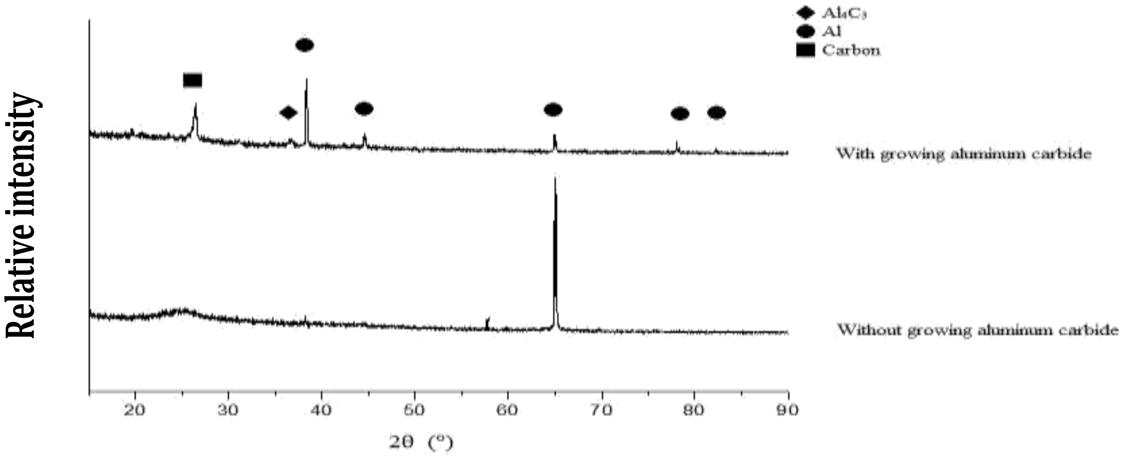

Figure 10: X-ray diffraction patterns of samples with and without aluminum carbide (grown with Al powder/C powder and CH_4 for 1 h at 540°C).

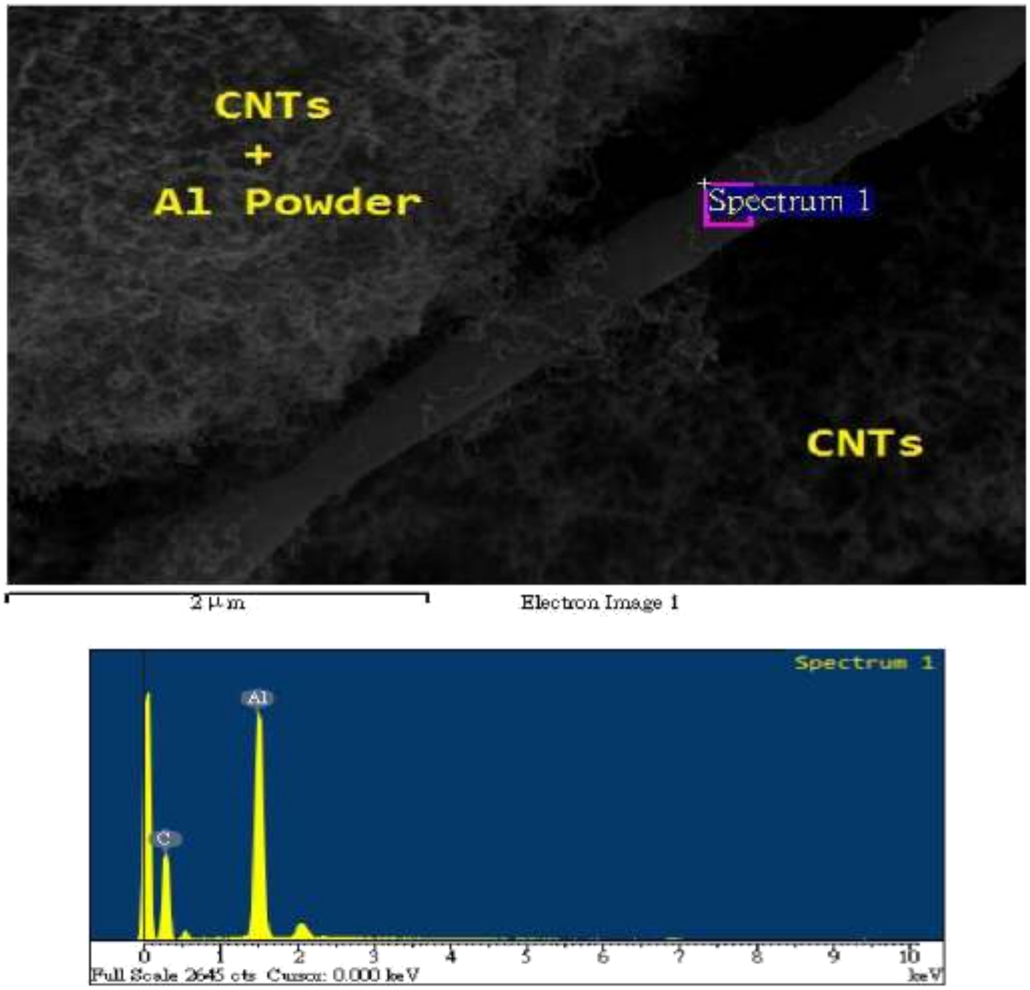

Figure 11: FE-SEM micrograph and EDX spectroscopy of aluminum carbide.

was lower than that without aluminum carbide (Figure 9) due to higher relative intensity (2Θ = 37.850) of Al_4C_3 for aluminum carbide grown (Figure 10).

FE-SEM of Figure 11 shows aluminum carbide

(Spectrum 1) formed as a result of chemical reaction between aluminum and carbon at the interface. According to EDX of Figure 11, a large amount of Al and a small amount of C were detected for Al_4C_3 (Spectrum 1).

Conclusion

Longer duration growth of aluminum carbide led to lower capacitance. The capacitance for aluminum carbide grown only with CH_4 was lower than that of others and the capacitance of capacitors with aluminum carbide was higher than those without aluminum carbide. Furthermore, the rate of decrease of capacitance of capacitors with aluminum carbide was lower than those without aluminum carbide. Moreover, FE-SEM combined with EDX shows aluminum carbide formed as the result of chemical reaction between aluminum and carbon at the interface.

ACKNOWLEDGEMENT

The authors are grateful to the National Science Council of the Republic of China (under grant no. NSC102－2221－E－224－047) for financial support rendered in the course of this research.

REFERENCES

Arik H, Ozcatalbas Y, Turker M (2006). Dry Sliding Wear Behavior of in Situ Al–Al_4C_3 Metal Matrix Composite Produced by Mechanical Alloying Technique. Materials and Design. 27(9):799-804.

Besterci M (2006). Kinetics of Carbonization, Microstructure and Properties of Al-Al_4C_3 System Prepared by Mechanical Alloying. J. Metals, Mater. Miner. 16(1):7-11.

Besterci M (2006). Preparation, Microstructure and Properties of Al–Al_4C_3 System Produced by Mechanical Alloying. Materials and Design. 27(5):416-421.

Birol Y (2008). Response to Thermal Exposure of the Mechanically Alloyed Al/C Powder Blends. J. Alloys Comp. 460(1-2):L1-L5.Chunfeng D, Xuexi Z, Dezun W (2007). Chemical Stability of Carbon Nanotubes in the 2024Al Matrix. Materials Letters. 61(3):904-907.

Ci L, Ryu Z, Jin-Phillipp NY, Ruhle M (2006). Investigation of the Interfacial Reaction between Multi-walled Carbon Nanotubes and Aluminum. Acta Materialia. 54(20):5367-5375.

Etter T, Schulz P, Weber M, Metzc J, Wimmler M, Löffler JF, Uggowitzer PJ (2007). Aluminum Carbide Formation in Interpenetrating Graphite/aluminum Composites. Materials Science and Engineering A. 448(1-2):1-6.

Goad DGW, Uchi H (2000). Modeling the Capacitance of d.c. Etched Aluminum Electrolytic Capacitor Foil. J. Appl. Electrochem. 30(3):285-291.

Guo L, Song W, Xie C, Zhang X, Hu M (2007). Characterization and Thermal Properties of Carbon-coated Aluminum Nanopowders Prepared by Laser-induction Complex Heating in Methane. Materials Lett. 61(14-15):3211-3214.

He CN, Zhao NQ, Shi CS, Song SZ (2009). Mechanical Properties and Microstructures of Carbon Nanotube-reinforced Al Matrix Composite Fabricated by in Situ Chemical Vapor Deposition. J. Alloys Comp. 487(1-2):258-262.

He CN, Zhao NQ, Shi CS, Song SZ (2010). Fabrication of Aluminum Carbide Nanowires by a Nano-template Reaction. Carbon. 48(4):931-938.

Kang J, Shin Y, Tak Y (2005). Growth of Etch Pits Formed during Sonoelectrochemical Etching of Aluminum. Electrochimica Acta. 51(5):1012-1016.

Kwon H, Park DH, Silvain JF, Kawasaki A (2010). Investigation of Carbon Nanotube Reinforced Aluminum Matrix Composite Materials. Composites Science and Technology. 70(3):546-550.

Liao J, Tan MJ (2011). Mixing of Carbon Nanotubes (CNTs) and Aluminum Powder for Powder Metallurgy Use. Powder Technology. 208(1):42-48.

Lu C, Ashitaka Z, Tada H, Arai S, Saka H (2004 a). Formation of Nano-scale Aluminum Carbide Whiskers on Aluminum Foil. In Proceedings of 206th Meeting, The Electrochemical Society, Inc. Abs. 262.

Lu C, Ashitaka Z, Tada H, Matsuda Y (2004 b). Electrochemical Characteristics of Aluminum Carbide Whisker. Kansai Daigaku Sangaku Renkei Kenkyu Senta Kenkyu Seika Hokokusho Heisei 16 Nendo. 191-192.

Poirier D, Gauvin R, Drew RAL (2009). Structural Characterization of a Mechanically Milled Carbon Nanotube/aluminum Mixture. Composites Part A: Applied Science and Manufacturing. 40(9):1482-1489.

Ro A, Ashitaka Z (2005). Carbon-Coated Aluminum and Method for Producing Same. European Patent EP 1 609 878 A1.

Ro A, Ashitaka Z, Tada H (2009). Electrode Material and Method for Producing Same. US Patent US 7,639,475 B2.

Sharifi EM, Enayati MH, Karimzadeh F (2012). Fabrication and Characterization of Al-Al_4C_3Nanocomposite by Mechanical Alloying. Int. J. Modern Phy. Conference Series. 5:480-487.

Sun Y, Cui H, Gong L, Chen J, She J, Ma Y, Shen P, Wang C (2011). Carbon-in-Al_4C_3Nanowire Superstructures for Field Emitters. ACS Nano. 5(2):932-941.

Xu CL, Wei BQ, Ma RZ, Liang J, Ma XK, Wu DH (1999). Fabrication of Aluminum–carbon Nanotube Composites and Their Electrical Properties. Carbon. 37(5):855-858.